# Unitarity effects in high-energy elastic scattering

Emerson Luna

*Instituto de Física*
*Universidade Federal do Rio Grande do Sul*

*XXXVII International Workshop on High Energy Physic*

*"Diffraction of hadrons: Experiment, Theory, Phenomenology"*

Protvino, Russia, 2025

## Outline

- Unitarization Schemes
  - $\Rightarrow$ Born amplitudes: Pomeron and Odderon inputs
- The tension between the TOTEM and ALFA/ATLAS measurements
- Results
- Conclusion and Perspectives

■ In order to describe the observed increase of $\sigma_{tot}(s)$, the Pomeron should have a supercritical intercept given by $\alpha_{\mathbb{P}}(0) = 1 + \epsilon$ with $\epsilon > 0$

$\Rightarrow$ the behavior of the total cross section for $\alpha_{\mathbb{P}}(0) > 1$ betokens the violation of the Froissart-Martin limit at some energy scale

■ It is expected that unitarity can be enforced in high-energy hadron-hadron interactions by the inclusion of the exchange series $\mathbb{P} + \mathbb{P}\mathbb{P} + \mathbb{P}\mathbb{P}\mathbb{P} + \ldots$

$\Rightarrow$ $\alpha_{\mathbb{P}}(0)$ is an effective power representing $n$-Pomeron exchange processes, $n \geq 1$

Despite the advances in understanding the nature of the Pomeron in the last decades, we still need to learn how to fully compute the contributions from multiple-Pomeron exchange processes with $n \geq 3$

On the other hand, it is well-established that some unitarization schemes sum appropriately rescattering diagrams representing the exchange of several particular multiparticle states

$\Rightarrow$ these schemes are primarily based on phenomenological arguments

$\Rightarrow$ they are effective procedures for taking into account many of the properties of unitarity in the $s$-channel or,

at the very least,

for preventing the Froissart-Martin bound for $\sigma_{tot}$ from being violated

■ We focus on two key unitarization schemes: the eikonal and the *U*-matrix approaches

## Unitarization Schemes

■ Certain distinctive features of the high-energy $\mathcal{A}(s,t)$ are better illuminated when examined in the impact parameter $b$-representation:

$$2\,\mathrm{Im}\,H(s,b) = |H(s,b)|^2 + G_{in}(s,b) \tag{1}$$

$\Rightarrow$ $G_{in}(s,b)$ is the inelastic overlap function

□ After the integration over two-dimensional impact parameter space:

$$\sigma_{tot}(s) = \sigma_{el}(s) + \sigma_{in}(s)$$

where

$$\sigma_{tot}(s) = \frac{4\pi}{s}\mathrm{Im}\,\mathcal{A}(s,t=0) = 2\pi\int_0^\infty b\,db\,2\,\mathrm{Im}H(s,b)$$

$$\sigma_{el}(s) = \frac{\pi}{s^2} \int_{-\infty}^{0} dt \, |\mathcal{A}(s,t)|^2 = 2\pi \int_0^\infty b \, db \, |H(s,b)|^2$$

$$\sigma_{in}(s) = 2\pi \int_0^\infty b \, db \, \left( 2 \, \mathrm{Im} H(s,b) - |H(s,b)|^2 \right)$$

□ After defining a function

$$\rho(s,b) = \frac{\mathrm{Re}\, H(s,b)}{\mathrm{Im}\, H(s,b)}$$

and solving the quadratic equation for $\mathrm{Im}\, H(s,b)$ resulting from (1):

$$\mathrm{Im}\, H(s,b) = \frac{1 \pm \sqrt{1 - (1+\rho^2)\, G_{in}(s,b)}}{1+\rho^2} \qquad (2)$$

$\Rightarrow$ We see that $G_{in}(s, b)$ must fit onto the interval

$$0 \leq G_{in}(s, b) \leq (1 + \rho^2)^{-1}$$

where we have required $\text{Im}\, H(s, b)$ be real.

■ The construction of unitarized scattering amplitudes relies on two formal steps:

Step 1. The choice of a Born term $\mathcal{F}(s, t)$ with the crossing-even and crossing-odd parts defined as

$$\mathcal{F}^{\pm}(s, t) = \frac{1}{2}\left[\mathcal{F}^{pp}(s, t) \pm \mathcal{F}^{\bar{p}p}(s, t)\right]$$

□ The correspondent crossing-even and crossing-odd Born amplitudes in $b$-space are given by

$$\chi^{\pm}(s,b) = \frac{1}{s}\int_0^{\infty} q\,dq\,J_0(bq)\mathcal{F}^{\pm}(s,-q^2)$$

Step 2. Consists of writing the scattering amplitude $H_{\bar{p}p}^{pp}(s,b)$ in terms of the Born amplitudes $\chi_{\bar{p}p}^{pp}(s,b)$

$\Rightarrow$ Once this is done, $\mathcal{A}_{\bar{p}p}^{pp}(s,t)$ is finally obtained from the inverse Fourier-Bessel transform of $H_{\bar{p}p}^{pp}(s,b)$:

$$\mathcal{A}_{\bar{p}p}^{pp}(s,t) = s\int_0^{\infty} b\,db\,J_0(bq)\,H_{\bar{p}p}^{pp}(s,b)$$

## Eikonal Unitarization

■ The eikonal unitarization corresponds to the solution of equation (2) with the minus sign

⇒ The eikonal scheme (Es) leads us to the relation

$$H(s,b) = i\left[1 - e^{i\chi(s,b)}\right]$$

so that

$$\mathcal{A}_{[Es]}(s,t) = is\int_0^\infty b\,db\,J_0(bq)\left[1 - e^{i\chi(s,b)}\right]$$

□ In the Es there is an upper limit on the imaginary part of $H(s,b)$,

$$0 \leq \mathrm{Im}H(s,b) \leq (1+\rho^2)^{-1}$$

# Eikonal Unitarization

□ Solving the Unitarity Eq. (1) for $G_{in}(s,b)$ in terms of $\chi(s,b)$ yields

$$G_{in}(s,b) = 1 - e^{-2\,\mathrm{Im}\,\chi(s,b)}$$

$\Rightarrow$ The positivity condition on $G_{in}(s,b)$ and the upper limit on $\mathrm{Im}H(s,b)$ restrict the imaginary part of $\chi(s,b)$ over

$$0 \leq \mathrm{Im}\chi(s,b) \leq -\frac{1}{2}\ln\left(\frac{\rho^2}{1+\rho^2}\right)$$

$\Rightarrow$ In the limit of a perfectly absorbing profile $H(s,b)$ and $\chi(s,b)$ are purely imaginary

$\Rightarrow$ In this limit we have the asymptotic result $\sigma_{el}/\sigma_{tot} = 1/2$

## *U*-matrix Unitarization

■ The *U*-matrix unitarization corresponds to the solution of the unitarity equation (2) with the plus sign

⇒ The *U*-matrix scheme (Us) leads us to the relation

$$H(s,b) = \frac{\chi(s,b)}{1 - i\chi(s,b)/2}$$

so that

$$\mathcal{A}_{[Us]}(s,t) = is \int_0^\infty b\, db\, J_0(bq) \left[ \frac{2\chi(s,b)}{\chi(s,b) + 2i} \right]$$

□ In the Us the $\mathrm{Im}H(s,b)$ is constrained to lie in the interval

$$(1+\rho^2)^{-1} \leq \mathrm{Im}H(s,b) \leq 2(1+\rho^2)^{-1}$$

# $U$-matrix Unitarization

□ In the black disc and $\rho \to 0$ limits we have

$$\mathrm{Im}H(s,b) = 2$$

and

$$|H(s,b)|^2 = 4$$

$\Rightarrow$ These results lead us to the asymptotic behavior $\sigma_{el}/\sigma_{tot} = 1$

$\Rightarrow$ Thus $H(s,b)$ may exceed the black disc limit in this approach

## Born Input Amplitudes

■ The input Born amplitudes are associated with Reggeon exchange amplitudes

⇒ The corresponding amplitudes in the *b*-space are given by

$$\chi_i(s,b) = \frac{1}{s}\int \frac{d^2q}{2\pi}\, e^{i\mathbf{q}\cdot\mathbf{b}}\, \mathcal{F}_i(s,t)$$

where $i = -, +, \mathbb{P}$, and $\mathbb{O}$.

⇒ The physical amplitudes in *b*-space are obtained by summing of all possible exchanges:

$$\chi^{pp}_{\bar{p}p}(s,b) = \chi_{\mathbb{P}}(s,b) + \chi_+(s,b) \pm \chi_-(s,b) \pm \xi_{\mathbb{O}}\chi_{\mathbb{O}}(s,b)$$

⇒ Here $\chi_+(s,b)$ ($\chi_-(s,b)$) is the $C=+1$ ($C=-1$) Reggeon contribution

⇒ $\chi_{\mathbb{P}}(s,b)$ ($\chi_{\mathbb{O}}(s,b)$) is the Pomeron (Odderon) contribution

⇒ $\xi_{\mathbb{O}}$ is the Odderon phase factor

□ $\xi_{\mathbb{O}}$ is associated with the positivity property

□ However, unlike Pomeron, the Odderon is not constrained by positivity requirements

From a theoretical standpoint, this implies that it is not possible to determine the phase of the Odderon mathematically

- Specifically, the Born amplitude for each single exchange is

$$\mathcal{F}_i(s,t) = \beta_i^2(t)\eta_i(t)\left(\frac{s}{s_0}\right)^{\alpha_i(t)}$$

$\Rightarrow$ $\beta_i^2(t)$ is the elastic proton-Reggeon vertex

$\Rightarrow$ $\alpha_i(t)$ is the Regge trajectory

$\Rightarrow$ $\eta_i(t) = -ie^{-i\frac{\pi}{2}\alpha_i(t)}$ is the odd-signature factor

$\Rightarrow$ $\eta_i(t) = -e^{-i\frac{\pi}{2}\alpha_i(t)}$ is the even-signature factor

$\Rightarrow$ $s_0 \equiv 1\ \mathrm{GeV}^2$ is an energy scale

■ For Reggeons with positive charge-conjugation:

$$\beta_+(t) = \beta_+(0)\exp(r_+ t/2)$$

and

$$\alpha_+(t) = 1 - \eta_+ + \alpha'_+ t$$

□ Similarly, the Reggeons with negative charge-conjugation are described by the parameters $\beta_-(0)$, $r_-$, $\eta_-$, and $\alpha'_-$

■ For Pomeron exchange we adopt

$$\alpha_{\mathbb{P}}(t) = \alpha_{\mathbb{P}}(0) + \alpha'_{\mathbb{P}} t + \frac{m_\pi^2}{32\pi^3} h(\tau)$$

where $\alpha_{\mathbb{P}}(0) = 1 + \epsilon$ and

$$h(\tau) = -\frac{4}{\tau} F_\pi^2(t) \left[ 2\tau - (1+\tau)^{3/2} \ln\left( \frac{\sqrt{1+\tau}+1}{\sqrt{1+\tau}-1} \right) + \ln\left( \frac{m^2}{m_\pi^2} \right) \right] \quad (3)$$

with $\epsilon > 0$, $\tau = 4m_\pi^2/|t|$, $m = 1$ GeV, and $m_\pi = 139.6$ MeV

$\Rightarrow$ $F_\pi(t)$ is the form factor of the pion-Pomeron vertex:

$$F_\pi(t) = \beta_\pi/(1 - t/a_1)$$

$\Rightarrow$ $\beta_\pi$ specifies the value of the pion-Pomeron coupling

$\Rightarrow$ we take the additive quark model relation $\beta_\pi/\beta_P(0) = 2/3$

The third term on the right-hand side of (3) corresponds to pion-loop insertions and is generated by $t$-channel unitarity

■ We investigated two different forms for the proton-Pomeron vertex

□ The first vertex, specifying our "Model I", is given by

$$\beta_{\mathbb{P}}(t) = \beta_{\mathbb{P}}(0) \exp\left(\frac{r_{\mathbb{P}} t}{2}\right)$$

□ The second proton-Pomeron vertex, referred to as "Model II", has the power-like form

$$\beta_{\mathbb{P}}(t) = \frac{\beta_{\mathbb{P}}(0)}{(1 - t/a_1)(1 - t/a_{\mathbb{P}})} \tag{4}$$

⇒ Note that the parameter $a_1$ in (4) is the same as the one in the expression for $F_\pi(t)$

⇒ we fix this parameter at $a_1 = m_\rho^2 = (0.776\,\text{GeV})^2$

The total cross section, the elastic differential cross section, and the $\rho$ parameter are expressed in terms of the physical amplitude $\mathcal{A}_{\bar{p}p}^{pp}(s,t)$,

$$\sigma_{tot}^{pp,\bar{p}p}(s) = \frac{4\pi}{s} \operatorname{Im} \mathcal{A}_{\bar{p}p}^{pp}(s, t=0)$$

$$\frac{d\sigma^{pp,\bar{p}p}}{dt}(s,t) = \frac{\pi}{s^2} \left| \mathcal{A}_{\bar{p}p}^{pp}(s,t) \right|^2$$

$$\rho^{pp,\bar{p}p}(s) = \frac{\operatorname{Re} \mathcal{A}_{\bar{p}p}^{pp}(s, t=0)}{\operatorname{Im} \mathcal{A}_{\bar{p}p}^{pp}(s, t=0)}$$

together with the replacements $\mathcal{A}_{\bar{p}p}^{pp}(s,t) = \mathcal{A}_{[Es]}^{pp,\bar{p}p}(s,t)$ or $\mathcal{A}_{[Us]}^{pp,\bar{p}p}(s,t)$, where

$$\mathcal{A}^{pp,\bar{p}p}_{[Es]}(s,t) = is \int_0^\infty b\,db\,J_0(bq)\left[1 - e^{i\chi^{pp}_{\bar{p}p}(s,b)}\right]$$

and

$$\mathcal{A}^{pp,\bar{p}p}_{[Us]}(s,t) = is \int_0^\infty b\,db\,J_0(bq)\left[\frac{2\chi^{pp}_{\bar{p}p}(s,b)}{\chi^{pp}_{\bar{p}p}(s,b) + 2i}\right]$$

# The Odderon input

■ The Born amplitude for the Odderon contribution is represented as

$$\mathcal{F}_{\mathbb{O}}(s,t) = \beta_{\mathbb{O}}^2(t)\,\eta_{\mathbb{O}}(t)\left(\frac{s}{s_0}\right)^{\alpha_{\mathbb{O}}(t)}$$

where $\eta_{\mathbb{O}}(t) = -ie^{-i\frac{\pi}{2}\alpha_{\mathbb{O}}(t)}$

□ In the formulation of "Model III", we employ an exponential form factor for the proton-Odderon vertex:

$$\beta_{\mathbb{O}}(t) = \beta_{\mathbb{O}}(0)\exp\left(\frac{r_{\mathbb{O}}t}{2}\right)$$

with $r_{\mathbb{O}} = r_{\mathbb{P}}/2$

# The Odderon input

□ In the formulation of "Model IV", we adopt the power-like form for the proton-Odderon vertex:

$$\beta_{\mathbb{O}}(t) = \frac{\beta_{\mathbb{O}}(0)}{(1 - t/m_\rho^2)(1 - t/a_{\mathbb{O}})}$$

with $a_{\mathbb{O}} = 2a_{\mathbb{P}}$

⇒ The relationship between $a_{\mathbb{O}}$ and $a_{\mathbb{P}}$ that must satisfy the constraint $a_{\mathbb{O}} \geq a_{\mathbb{P}}$ to avoid non-physical amplitudes when using a power-like form factor

## The Odderon input

■ From the standpoint of QCD (at the lowest order) the $C = +1$ amplitude arises from the exchange of two gluons and the $C = -1$ amplitude from the exchange of three gluons

■ Extensive theoretical studies have been directed towards uncovering corrections to these results, particularly in higher orders

□ In this scenario, the leading-log approximation allows for the summation of certain higher-order contributions to physical observables in high-energy particle scattering processes

$\Rightarrow$ This approach was widely used in the study of the QCD-Pomeron through the BFKL equation

## The Odderon input

⇒ In BFKL equation terms of the order $(\alpha_s \ln(s))^n$ are systematically summed at high energy (large $s$) and small strong coupling $\alpha_s$

⇒ The simplistic notion of bare two-gluon exchange gives way to the BFKL Pomeron, which, in an alternative representation, can be seen as the interaction of two reggeized gluons with one another

■ Beyond the BFKL Pomeron, the most elementary entity within perturbative QCD is the exchange involving three interacting reggeized gluons

□ The evolution of the three-gluon Odderon exchange as energy increases is governed by the BKP equation

⇒ A bound state solution of this Odderon equation was obtained with the intercept $\alpha_{\mathbb{O}}(0) = 1$

# The Odderon input

- Based on these QCD findings, we adopt in this work the simplest conceivable form for the Odderon trajectory:

$$\alpha_{\mathbb{O}}(t) = 1$$

# Results

■ The LHC has released exceptionally precise measurements of diffractive processes

□ These measurements, particularly the total and differential cross sections obtained from ATLAS and TOTEM Collaborations, enable us to determine the Pomeron and Odderon parameters accurately

$\Rightarrow$ However, these experimental results unveil a noteworthy tension between the TOTEM and ATLAS measurements

$\Rightarrow$ For instance, when comparing the TOTEM and the ATLAS result for $\sigma_{tot}^{pp}$ at $\sqrt{s} = 8$ TeV, the discrepancy between the values corresponds to 2.6 $\sigma$

## Results

■ In order to systematically explore the tension between TOTEM and ATLAS results, we perform global fits to $pp$ and $\bar{p}p$ forward scattering data and to $pp$ differential cross-section data while considering two distinct datasets, one with TOTEM measurements and the other with ATLAS measurements

□ The two data ensembles can be defined as follows:
**Ensemble A**: $\sigma_{tot}^{pp,\bar{p}p}$ data + $\rho^{pp,\bar{p}p}$ data + ATLAS data on $\frac{d\sigma}{dt}$ at 7, 8, and 13 TeV;
**Ensemble T**: $\sigma_{tot}^{pp,\bar{p}p}$ data + $\rho^{pp,\bar{p}p}$ data + TOTEM data on $\frac{d\sigma}{dt}$ at 7, 8, and 13 TeV

⇒ We carry out global fits to the two distinct ensembles using a $\chi^2$ fitting procedure, where $\chi^2_{min}$ follows a $\chi^2$ distribution with $\nu$ DoF

⇒ We adopt an interval $\chi^2 - \chi^2_{min}$ corresponding to a 90% confidence level (CL).

# Pomeron Analysis

**Table:** The Pomeron and secondary Reggeons parameters values obtained in global fits to Ensembles A and T after the eikonal unitarization.

| | Ensemble A | | Ensemble T | |
|---|---|---|---|---|
| | Model I | Model II | Model I | Model II |
| $\epsilon$ | 0.1014±0.0033 | 0.1112±0.0013 | 0.1248±0.0027 | 0.1336±0.0023 |
| $\alpha'_{\boldsymbol{P}}$ (GeV$^{-2}$) | 0.2938±0.0022 | 0.1148±0.0076 | $0.56 \times 10^{-9}$ ±0.11 | 0.009±0.040 |
| $\beta_{\mathbb{P}}(0)$ | 2.154±0.063 | 1.999±0.023 | 1.814±0.043 | 1.742±0.028 |
| $r_{\mathbb{P}}$ (GeV$^{-2}$) | 2.375±0.019 | — | 7.448±0.087 | — |
| $a_{\mathbb{P}}$ (GeV$^{-2}$) | — | 0.829±0.081 | — | 0.499±0.084 |
| $\eta_+$ | 0.360±0.048 | 0.344±0.030 | 0.286±0.025 | 0.262±0.015 |
| $\beta_+(0)$ | 4.56±0.47 | 4.37±0.34 | 4.02±0.21 | 3.93±0.14 |
| $\eta_-$ | 0.556±0.010 | 0.550±0.089 | 0.536±0.067 | 0.530±0.064 |
| $\beta_-(0)$ | 3.68±0.16 | 3.55±0.67 | 3.41±0.49 | 3.39±0.46 |
| $\nu$ | 226 | 226 | 350 | 350 |
| $\chi^2/\nu$ | 0.86 | 0.83 | 0.74 | 0.65 |

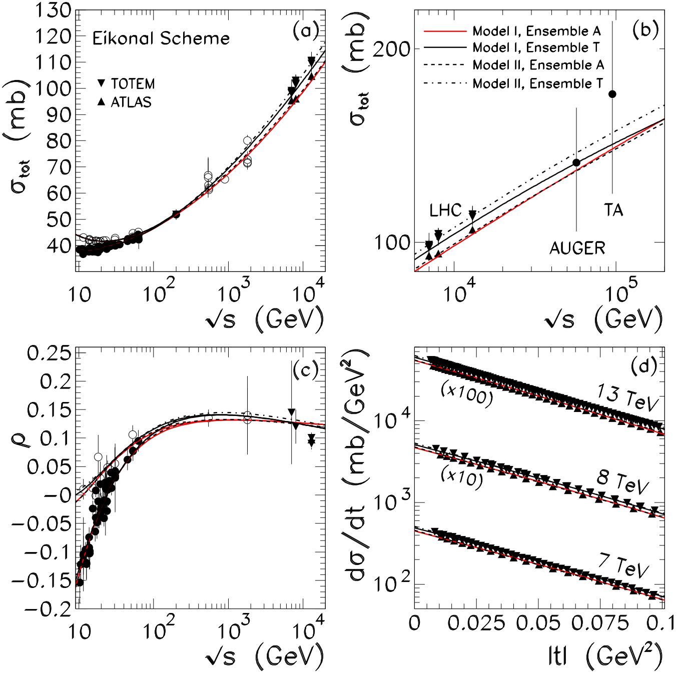

Eikonal Scheme
(a)
TOTEM
ATLAS
$\sigma_{tot}$ (mb)
$\sqrt{s}$ (GeV)
Model I, Ensemble A
Model I, Ensemble T
Model II, Ensemble A
Model II, Ensemble T
(b)
LHC
TA
AUGER
(c)
$\rho$
(d)
(x100)
13 TeV
(x10)
8 TeV
7 TeV
$d\sigma/dt$ (mb/GeV$^2$)
|t| (GeV$^2$)

## Pomeron Analysis

**Table:** The Pomeron and secondary Reggeons parameters values obtained in global fits to Ensembles A and T after the *U*-matrix unitarization.

| | Ensemble A | | Ensemble T | |
|---|---|---|---|---|
| | Model I | Model II | Model I | Model II |
| $\epsilon$ | 0.0911±0.0037 | 0.0981±0.0029 | 0.1129±0.0048 | 0.1150±0.0070 |
| $\alpha'_{\mathbb{P}}$ (GeV$^{-2}$) | 0.4425±0.0085 | 0.2728±0.0089 | 0.05±0.14 | 0.10±0.12 |
| $\beta_{\mathbb{P}}(0)$ | 2.271±0.075 | 2.140±0.056 | 1.926±0.085 | 1.92±0.11 |
| $r_{\mathbb{P}}$ (GeV$^{-2}$) | 0.1051±0.0061 | — | 7.2±2.8 | — |
| $a_{\mathbb{P}}$ (GeV$^{-2}$) | — | 40±20 | — | 0.62±0.49 |
| $\eta_+$ | 0.356±0.057 | 0.369±0.049 | 0.325±0.050 | 0.314±0.053 |
| $\beta_+(0)$ | 4.71±0.65 | 4.51±0.48 | 4.18±0.43 | 4.14±0.44 |
| $\eta_-$ | 0.551±0.098 | 0.551±0.043 | 0.545±0.074 | 0.542±0.075 |
| $\beta_-(0)$ | 3.59±0.74 | 3.54±0.34 | 3.43±0.54 | 3.43±0.54 |
| $\nu$ | 226 | 226 | 350 | 350 |
| $\chi^2/\nu$ | 0.85 | 0.86 | 0.71 | 0.64 |

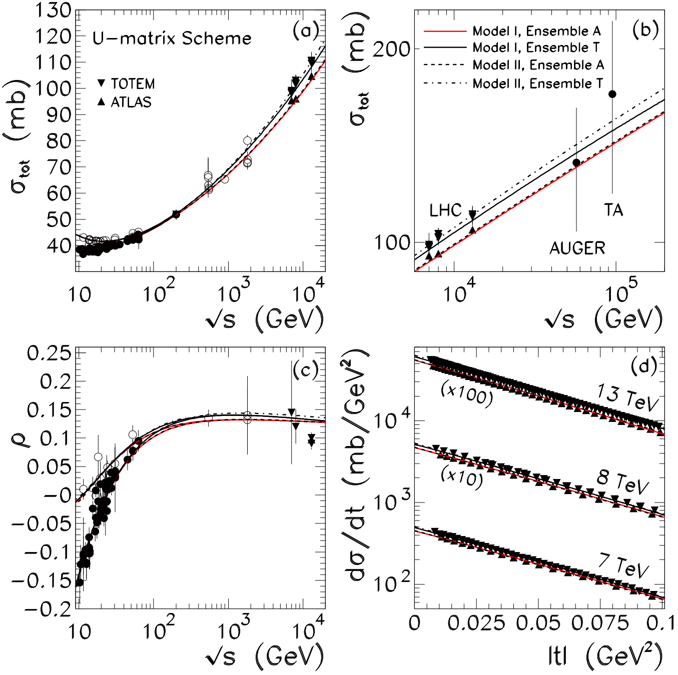
U−matrix Scheme
(a)
TOTEM
ATLAS
σtot (mb)
√s (GeV)
(b)
Model I, Ensemble A
Model I, Ensemble T
Model II, Ensemble A
Model II, Ensemble T
LHC
AUGER
TA
(c)
ρ
(d)
(x100)
13 TeV
(x10)
8 TeV
7 TeV
dσ/dt (mb/GeV²)
|t| (GeV²)

# Pomeron $\oplus$ Odderon Analysis

**Table:** The Pomeron, Odderon and secondary Reggeons parameters values obtained in global fits to Ensembles A and T after the eikonal unitarization. We show the results with $\xi_{\mathbb{O}} = -1$.

| | Ensemble A | | Ensemble T | |
|---|---|---|---|---|
| | Model III | Model IV | Model III | Model IV |
| $\epsilon$ | 0.1017±0.0043 | 0.1043±0.0026 | 0.1247±0.0048 | 0.1335±0.0041 |
| $\alpha'_{P}$ (GeV$^{-2}$) | 0.283±0.036 | 0.242±0.012 | $0.94 \times 10^{-4}$ ±0.059 | 0.01±0.11 |
| $\beta_{\mathbb{P}}(0)$ | 2.146±0.083 | 2.116±0.011 | 1.815±0.080 | 1.744±0.035 |
| $r_{\mathbb{P}}$ (GeV$^{-2}$) | 2.58±0.68 | — | 7.45±0.13 | — |
| $a_{\mathbb{P}}$ (GeV$^{-2}$) | — | 31±11 | — | 0.50±0.16 |
| $\beta_{\mathbb{O}}(0)$ | 0.47±0.24 | 0.40±0.17 | 0.31±0.24 | 0.27±0.20 |
| $\eta_{+}$ | 0.359±0.055 | 0.353±0.020 | 0.285±0.051 | 0.261±0.013 |
| $\beta_{+}(0)$ | 4.52±0.54 | 4.47±0.29 | 4.00±0.38 | 3.91±0.16 |
| $\eta_{-}$ | 0.4823±0.0019 | 0.482±0.077 | 0.490±0.030 | 0.489±0.077 |
| $\beta_{-}(0)$ | 3.20±0.13 | 3.19±0.50 | 3.14±0.22 | 3.15±0.50 |
| $\nu$ | 225 | 225 | 349 | 349 |
| $\chi^2/\nu$ | 0.84 | 0.80 | 0.73 | 0.65 |

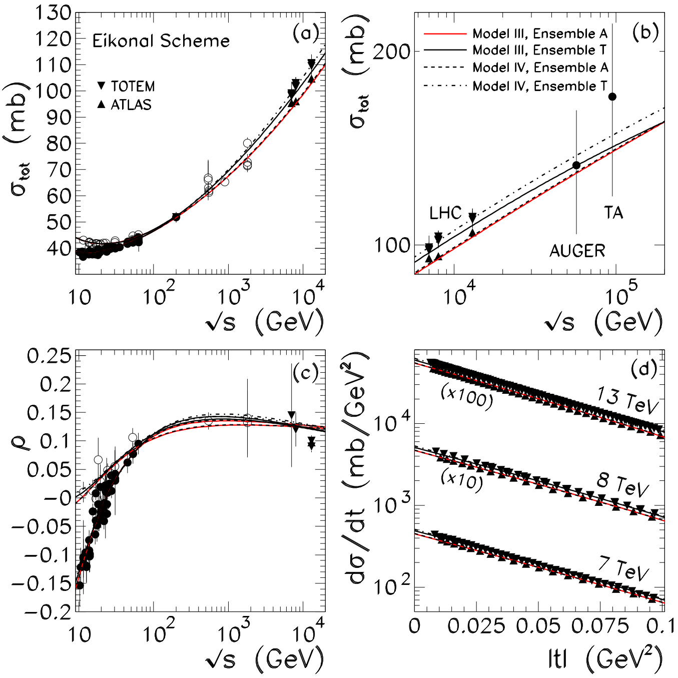
Eikonal Scheme
(a)
TOTEM
ATLAS
$\sigma_{tot}$ (mb)
$\sqrt{s}$ (GeV)
(b)
Model III, Ensemble A
Model III, Ensemble T
Model IV, Ensemble A
Model IV, Ensemble T
LHC
AUGER
TA
(c)
$\rho$
(d)
(x100)
13 TeV
(x10)
8 TeV
7 TeV
$d\sigma/dt$ (mb/GeV$^2$)
|t| (GeV$^2$)

# Pomeron $\oplus$ Odderon Analysis

**Table:** The Pomeron, Odderon and secondary Reggeons parameters values obtained in global fits to Ensembles A and T after the *U*-matrix unitarization. We show the results with $\xi_{\mathbb{O}} = -1$.

| | Ensemble A | | Ensemble T | |
|---|---|---|---|---|
| | Model III | Model IV | Model III | Model IV |
| $\epsilon$ | 0.0938±0.0045 | 0.0978±0.0047 | 0.1115±0.0035 | 0.1148±0.0060 |
| $\alpha'_{\mathbb{P}}$ (GeV$^{-2}$) | 0.364±0.029 | 0.273±0.031 | 0.10±0.15 | 0.106±0.098 |
| $\beta_{\mathbb{P}}(0)$ | 2.215±0.075 | 2.146±0.066 | 1.951±0.063 | 1.919±0.093 |
| $r_{\mathbb{P}}$ (GeV$^{-2}$) | 1.57±0.58 | — | 6.2±3.0 | — |
| $a_{\mathbb{P}}$ (GeV$^{-2}$) | — | 40±24 | — | 0.63±0.41 |
| $\beta_{\mathbb{O}}(0)$ | 0.44±0.20 | 0.23±0.15 | 0.32±0.18 | 0.27±0.18 |
| $\eta_+$ | 0.374±0.031 | 0.369±0.026 | 0.327±0.071 | 0.313±0.046 |
| $\beta_+(0)$ | 4.62±0.50 | 4.49±0.64 | 4.18±0.72 | 4.12±0.38 |
| $\eta_-$ | 0.490±0.047 | 0.48±0.33 | 0.49±0.21 | 0.50±0.12 |
| $\beta_-(0)$ | 3.18±0.18 | 3.08±0.79 | 3.11±0.42 | 3.17±0.71 |
| $\nu$ | 225 | 225 | 349 | 349 |
| $\chi^2/\nu$ | 0.83 | 0.84 | 0.71 | 0.64 |

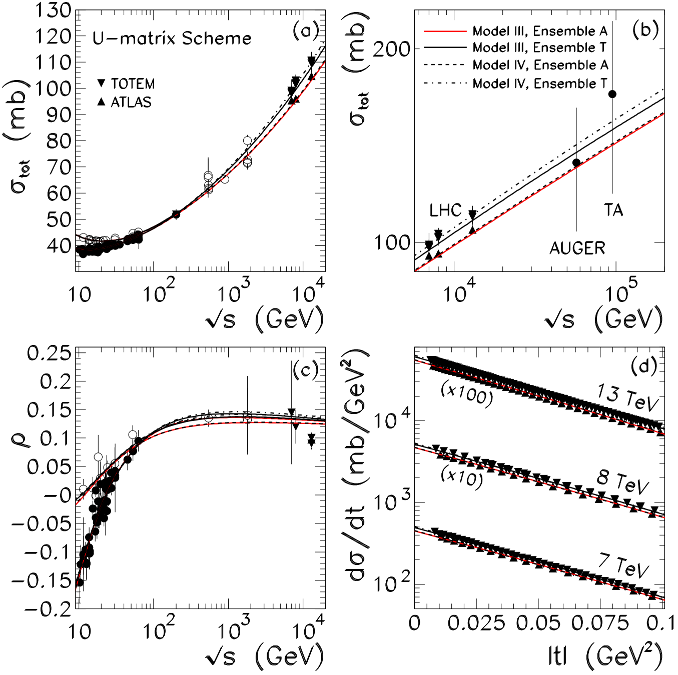
U−matrix Scheme
(a)
TOTEM
ATLAS
σ_tot (mb)
√s (GeV)
(b)
Model III, Ensemble A
Model III, Ensemble T
Model IV, Ensemble A
Model IV, Ensemble T
LHC
TA
AUGER
σ_tot (mb)
√s (GeV)
(c)
ρ
√s (GeV)
(d)
(x100)
13 TeV
(x10)
8 TeV
7 TeV
dσ/dt (mb/GeV²)
|t| (GeV²)

# Conclusions and Perspectives

■ The presence of the Odderon immediately impacts the behavior of total cross sections, particularly generating different growth patterns for $\sigma_{tot}^{pp}(s)$ and $\sigma_{tot}^{\bar{p}p}(s)$ at high energies

$\Rightarrow$ With an asymptotic non-zero crossing-odd term $\mathcal{A}^{-}(s,t)$ in the scattering amplitude, it is possible to demonstrate that $|\Delta\sigma|$ can be at most $|\Delta\sigma| = k \ln s$ in the limit $s \to \infty$, where $k$ is a constant

■ After introducing the Odderon, the eikonal scheme demonstrates a slight advantage over the $U$-matrix scheme, mirroring the scenario where the Pomeron is the sole asymptotically dominant entity

■ We observe that for an Odderon with a phase factor $\xi_{\mathbb{O}} = +1$, all eight $\beta_{\mathbb{O}}(0)$ values obtained are consistent with zero (errors significantly surpassing central values)

# Conclusions and Perspectives

$\Rightarrow$ Consequently, the remaining parameters assume values very closely resembling the scenario where the Pomeron dominates the scattering amplitude

- The Odderon phase is well-defined and is equal to $\xi_{\mathbb{O}} = -1$

- An ongoing analysis focusing solely on high-energy data, considering exclusively the contributions from Pomeron and Odderon, is imperative to ascertain the stability of the Odderon phase factor

- Ongoing investigations involving a two-channel model are underway, focusing on the study of eikonal and *U*-matrix unitarization schemes within the context of our analysis

THANK YOU

# Resummations in QCD

■ Every physical observable can be written, in pQCD, as a power series in $\alpha_s$

$\Longrightarrow$ in these series the coupling constant is accompanied by large logarithms, which need to be resummed

$\Longrightarrow$ according to the type and to the powers of logarithms that are effectively resummed one gets different evolution equations

■ The solution of the DGLAP equation sums over all orders in $\alpha_s$ the contributions from leading, single, collinear logarithms of the form $\alpha_s \ln\left(Q^2/Q_0^2\right)$

$\Longrightarrow$ it does not include leading, single, soft singularities of the form $\alpha_s \ln\left(1/x\right)$, which are treated instead by the BFKL equation

■ The BFKL equation describes the $x$-evolution of PDFs at fixed $Q^2$

## Resummations in QCD

■ The phase space regions which contribute these logarithms enhancements are associated with configurations in which successive partons have strongly ordered transverse, $k_T$, or longitudinal, $k_L \equiv x$, momenta:

$\Rightarrow \alpha_s L_Q \sim 1$, $\alpha_s L_x \ll 1$: $Q^2 \gg k^2_{T,n} \gg \cdots \gg k^2_{T,1} \gg Q^2_0$

$\Rightarrow \alpha_s L_x \sim 1$, $\alpha_s L_Q \ll 1$: $x \ll x_n \ll \cdots \ll x_1 \ll x_0$

■ At small-$x$ and slow $Q^2$ (where gluons are dominant) we do not have strongly ordered $k_T$

$\Rightarrow$ we have to integrate over the full range of $k_T$

$\Rightarrow$ this leads us to work with the *unintegrated* gluon PDF $\tilde{g}(x, k_T^2)$:

$$xg(x, Q^2) = \int^{Q^2} \frac{dk_T^2}{k_T^2} \tilde{g}(x, k_T^2)$$

# Positivity

■ The phase factor is associated with the positivity property

$\Rightarrow$ However, unlike Pomeron, the Odderon is not constrained by positivity requirements

$\Rightarrow$ From a theoretical standpoint, this implies that it is not possible to determine the phase of the Odderon mathematically

□ This issue can be succinctly grasped: in the forward direction the physical amplitudes $\mathcal{F}^{pp}_{\bar{p}p}(s)$ can be written as $\mathcal{F}^{pp}_{\bar{p}p}(s) = F^{+}(s) \pm F^{-}(s)$

□ Considering that the only relevant contributions are those arising from the Pomeron and the Odderon exchanges, we can write the symmetric and antisymmetric amplitudes as $F^{+}(s) = R_{\mathbb{P}}(s) + iI_{\mathbb{P}}(s)$ and $F^{-}(s) = R_{\mathbb{O}}(s) + iI_{\mathbb{O}}(s)$

□ From the optical theorem, we have $s\sigma_{tot}^{pp,\bar{p}p}(s) = 4\pi \,\mathrm{Im}\,\mathcal{F}_{\bar{p}p}^{pp}(s) > 0$, which implies that

$$\mathrm{Im}\,\mathcal{F}_{\bar{p}p}^{pp}(s) = I_{\mathbb{P}}(s) \pm I_{\mathbb{O}}(s) > 0$$

and, in turn,

$$I_{\mathbb{P}}(s) > |I_{\mathbb{O}}(s)|$$

As a consequence,

$$I_{\mathbb{P}}(s) = \frac{s}{2}\left[\sigma_{tot}^{pp}(s) + \sigma_{tot}^{\bar{p}p}(s)\right] > 0$$

while

$$I_{\mathbb{O}}(s) = \frac{s}{2}\left[\sigma_{tot}^{pp}(s) - \sigma_{tot}^{\bar{p}p}(s)\right]$$

is not bound by the same positivity requirements